CNRS
Centre National de la Recherche Scientifique

INFN
Istituto Nazionale di Fisica Nucleare

Convergence of modal simulations of MSRC

VIR-0292A-10

Gabriele Vajente
INFN sezione di Pisa and Pisa University

Issue: 1

Date: May 4, 2010

VIRGO * A joint CNRS-INFN Project
Via E. Amaldi, I-56021 S. Stefano a Macerata - Cascina (Pisa)
Secretariat: Telephone (39) 050 752 521 * FAX (39) 050 752 550 * Email W3@virgo.infn.it

Contents

1 Introduction

Modal simulation of Advanced Virgo marginally stable recycling cavities have been carried out using a limited number of transverse modes ($n + m \leq 8$) [1, 2, 3]. This choice was normally good in simulating Virgo-like configuration, but it was discovered that it was not sufficient in the Advanced Virgo configuration [4, 5].

Thermal effects in modal simulations are described introducing a mode coupling matrix in input of the arm cavities which describes the effect of the thermally induced lens. It can be easily shown that with the same absorbed power the coupling matrix is independent of the beam size. Indeed the matrix is computed from the scalar product of the perturbed field with the initial one:

$$M_{mn,pq} = \int\int \psi^*_{pq}(x,y) e^{k\frac{x^2+y^2}{2f}} \psi_{mn}(x,y)\,\mathrm{dxdy} \tag{1.1}$$

being (m,n) the indexes of the input mode and (p,q) of the output one and f the focal length of the lens. Using the explicit form of the modes

$$\psi_{mn} = \sqrt{\frac{2}{\pi}}\sqrt{\frac{1}{2^{n+m}m!n!w^2(z)}} H_m\left(\frac{\sqrt{2}}{w(z)}x\right) H_n\left(\frac{\sqrt{2}}{w(z)}y\right) \exp\left[-(x^2+y^2)\left(\frac{1}{w^2(z)} + \frac{ik}{2R(z)}\right)\right] \tag{1.2}$$

and performing a change of integration variable one gets:

$$\begin{aligned} M_{mn,pq} \quad \propto \quad & \frac{1}{w^2(z)} w^2(z) \int\int H_p(\chi)\, H_q(\zeta)\, H_m(\chi)\, H_n(\zeta) \\ & e^{-(\chi^2+\zeta^2)} e^{ik(\chi^2+\zeta^2)\frac{w^2(z)}{2f}}\,\mathrm{d}\chi\mathrm{d}\zeta \end{aligned}$$

where the first w^2 factor comes from the mode normalization and the second one from the change of variable. The integral depends on the beam size only inside the exponent with the term $w^2(z)/2f$. Analytical models and finite element analysis [6] showed that the focal length scales as

$$f = \frac{\alpha w^2}{P_{ABS}} \tag{1.3}$$

where the constant α is independent on the beam size. In conclusion the coupling matrix is independent of the beam size.

Nevertheless a different behavior is observed between the Virgo and Advanced Virgo power recycling cavities: the latter are more sensitive to thermal effects or in other words the sideband recycling gain is normally significantly smaller. Moreover using modes only up to $n + m \leq 8$ is sufficient in the Virgo case but clearly not enough for Advanced Virgo. This difference can be explained considering that the different beam geometry is such to have different Gouy phases in the recycling cavity. In the Advanced Virgo case the input and power recycling mirrors are placed in far field and the Gouy phase accumulated in propagation is very small, about 0.08 degrees. Instead in the Virgo configuration the input and power recycling mirror are placed in near field and the Rayleigh length is small enough to make the Gouy phase about 0.5 degrees. This is enough to move large order modes out

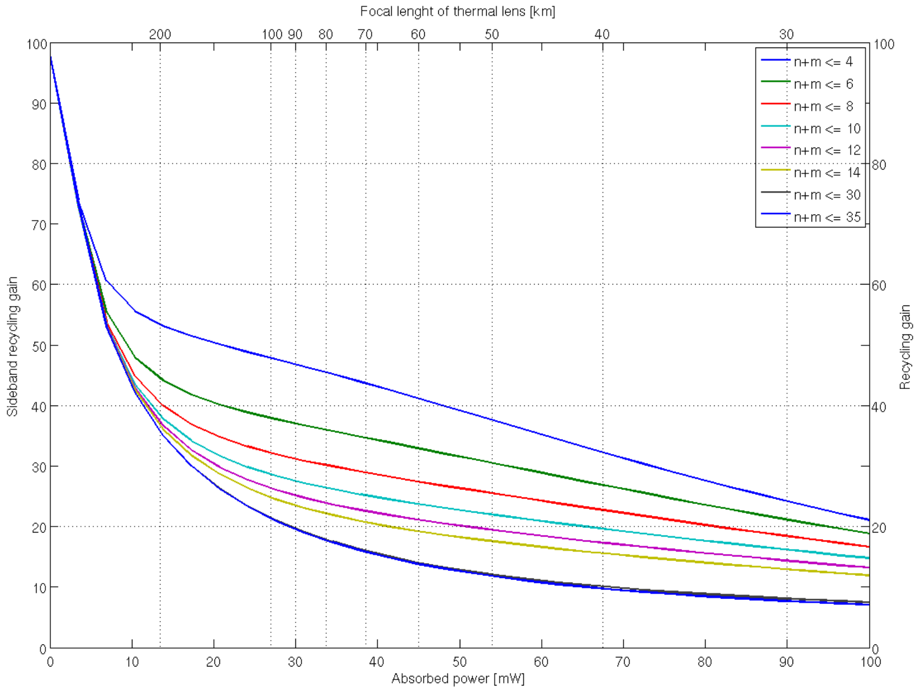

Figure 1: Comparison of the simulation outcome with different maximum number of modes. Here the sideband recycling gain is shown.

of PRC resonance. This explains both the lower sensitivity to thermal effects and the lower number of modes needed to have consistent results in the simulation.

This note analyzes the problem of convergence of modal simulations of Advanced Virgo MSRC. All simulation parameters are the same explained for example in [2, 3]. Section 2 studies the effect on sideband recycling gain, and section 3 on the detector response to differential strain.

2 Sideband recycling gain

The main effect of thermal lensing in the input substrate is a reduction of the radio-frequency sideband recycling gain. In the Advanced Virgo MSRC configuration the previous modal simulation were performed using $n+m \leq 8$ [2]. This turned out to be not enough [4], since the coupling into large order modes, which are still resonant inside PRC, was very important.

Figure 1 shows how the simulated sideband recycling gain changes with the maximum number of modes used (see also [4]). It is clear that 8 was not sufficient, except for small lensings. It appears also clear that the convergence of the modal simulation is not the same for all focal lengths, being slower for larger lenses.

To better understand the convergence speed of the simulation, sideband recycling gain has been simulated for two different lensings (70 km and 20 km) with varying number of modes (see fig. 2). It appears that the convergence is exponential. Moreover, for 70 km the convergence is good already for $m + n \leq 30$, while for 20 km one need to use at least $n + m \leq 50$ or larger.

A similar comparison has also been done with a Virgo-like configuration, which means small beams in the input mirrors and a Gouy phase of 0.5 degrees in the PRC, see fig. 3. Cavity finesse and power recycling reflectivity were maintained the same as in the Advanced Virgo configuration. It appears clear that a much smaller number

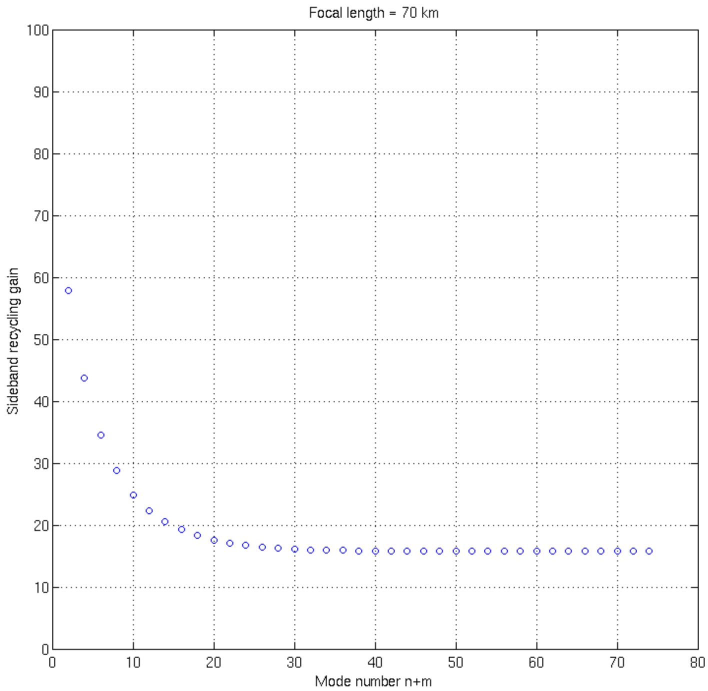

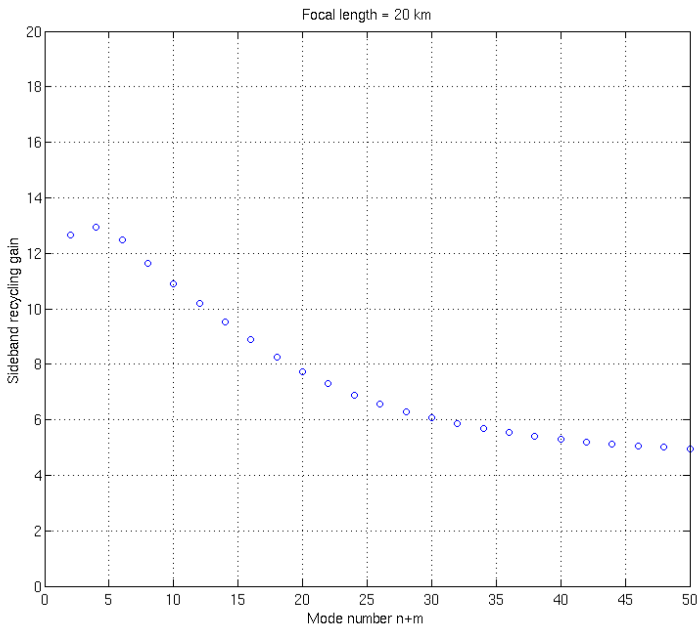

Figure 2: Convergence of sideband recycling gain for modal simulation, as a function of the maximum number of modes used. The top plot is for a focal length of 70 km, while the bottom one for 20 km.

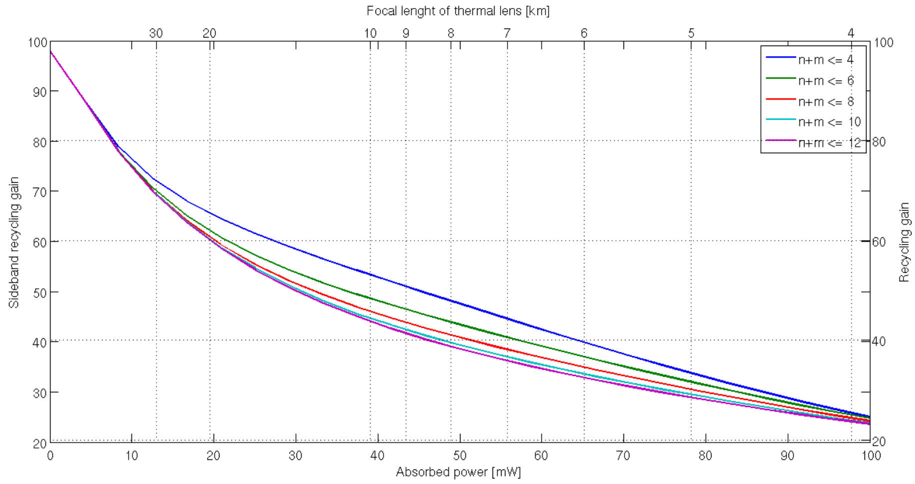

Figure 3: Comparison of the simulation outcome with different maximum number of modes. A Virgo-like geometry has been used here.

of modes is needed to reach convergence of the simulation. Indeed the difference between 8 and 10 is already small.

3 Detector response to differential strain

Changing the maximum number of modes has also an effect on the detector response to differential motion of the end mirror (gravitational waves). The effect was expected to be small, since signal sidebands partially resonate also inside the arm cavities and therefore high order modes should be distinguished from the fundamental one.

Indeed figures 4 and 5 show that the transfer function from differential motion of the end mirrors to dark port signal does not change significantly with increasing number of modes and it is indeed stable after $n + m \leq 8$. The result shown there have been computed for a focal length of 70 km.

Figure 6 shows more in detail that the convergence of the transfer function is quite fast with the number of modes and the difference with respect to the final value is already within 1% for $n + m \leq 8$.

4 Conclusions

Modal simulations of marginally stable recycling cavities in the Advanced Virgo geometry need a large number of modes to give consistent results, at least for what concern the sideband recycling gain. The results shown for example in [2] were computed using $n + m \leq 8$ which is not enough. Indeed depending on the focal length of the thermal lens, the needed number of modes can become quite large. For 70 km $n + m$ should be at least 30, while for 20 km for example it must be larger than 50. With respect to what presented in [2] the final sideband recycling gain (for 70 km) is about a factor 2 lower.

The situation is different for what concerns the detector response to differential strain. Since audio sidebands are partially resonating inside the arms, high order modes are less important and indeed already with $n+m \leq 8$ results are within 1% of the final result.

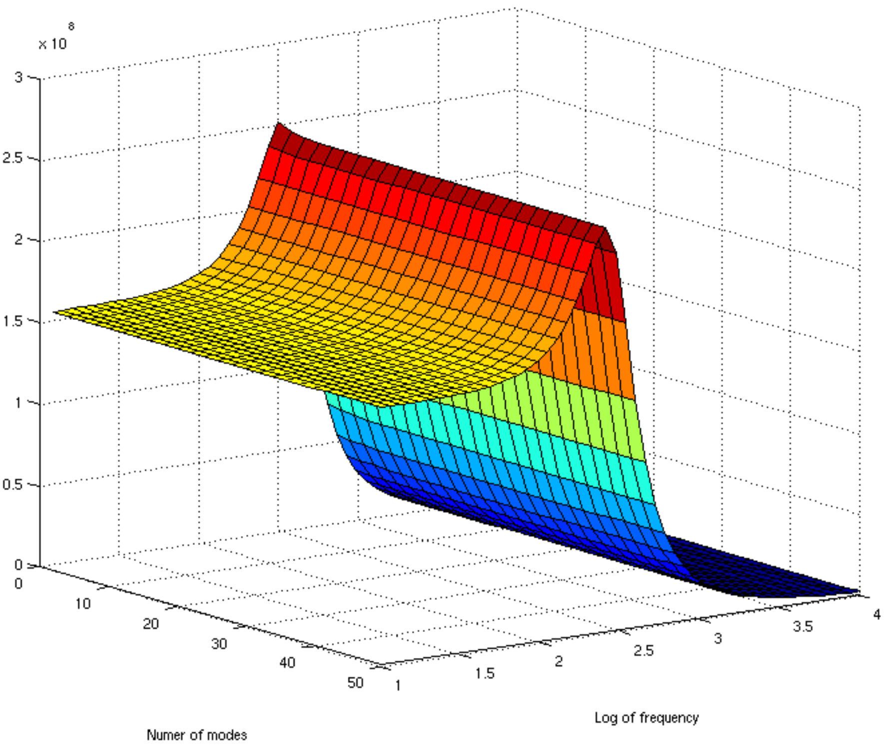

Figure 4: Detector response to a differential motion of the end mirrors as a function of frequency and maximum number of modes. The focal length of the thermal lens is 70 km.

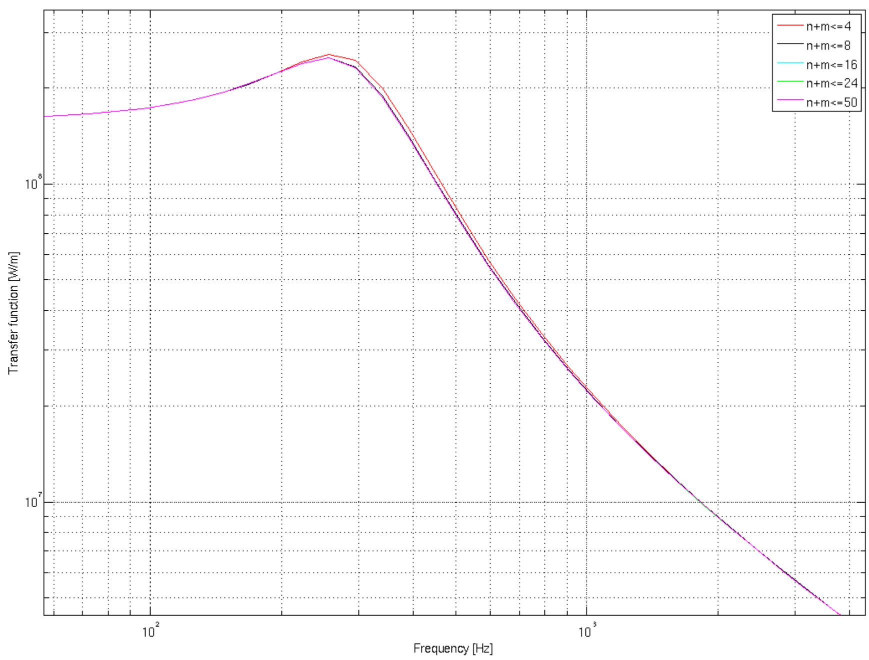

Figure 5: Detector response to a differential motion of the end mirrors as a function of frequency and maximum number of modes. The focal length of the thermal lens is 70 km.

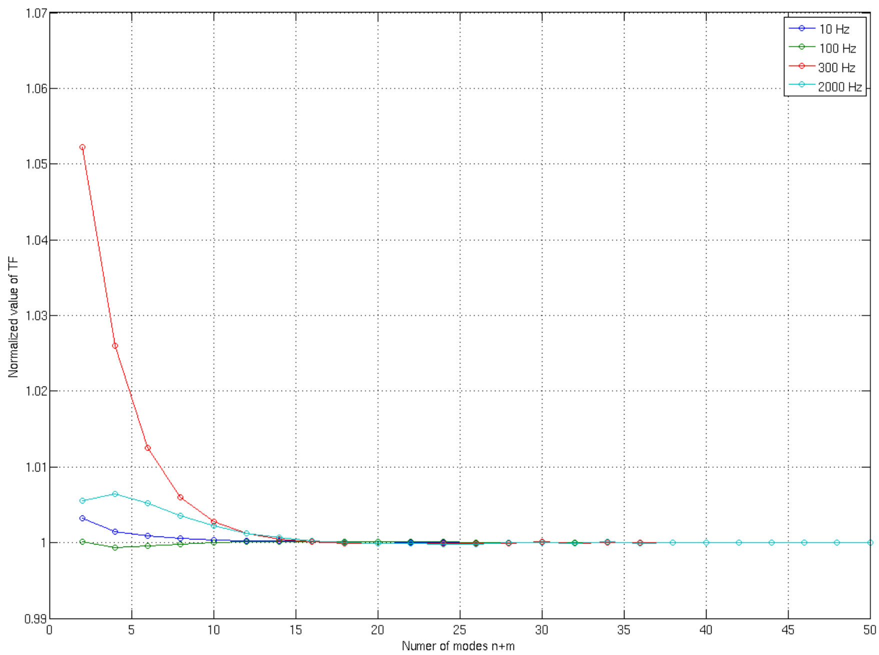

Figure 6: Detector response to a differential motion of the end mirrors as a function of the maximum number of modes for few frequencies.

References

[1] G. Vajente, *Modal Interferometer Simulation*, VIR-0142A-10 (2010) 1

[2] G. Vajente, J. Marque, *Simulations of Advanced Virgo recycling cavities and thermal effects*, VIR-0148A-10 (2010) 1, 2, 4

[3] G. Vajente, J. Marque, *Simulations of Advanced Virgo recycling cavities and thermal effects - Part 2*, VIR-0167A-10 (2010) 1, 2

[4] R. Flaminio, R. Bonnand, *Simulation of Thermal Effects in Adv. Virgo*, VIR-0267A-10 (2010) 1, 2

[5] H. Yamamoto, *Marginally stable cavity simulation : FFT vs Modal Model*, VIR-0261-A (2010) 1

[6] R. Day *et al. Virgo Input Mirrors thermal effects characterization*, VIR-0191A-10 (2010) 1